HHS Public Access

Author manuscript

Cells Tissues Organs. Author manuscript; available in PMC 2022 September 09.

Published in final edited form as:

Cells Tissues Organs. 2021 ; 210(4): 301–310. doi:10.1159/000517622.

A Two-Step Bioreactor for Decellularized Lung Epithelialization

Bethany M. Young[1], **Leigh-Ann M. Antczak**[1], **Keerthana Shankar**[1], **Rebecca L. Heise**[*,1,2]

[1]Department of Biomedical Engineering, Virginia Commonwealth University, 70 S. Madison St, Richmond, VA 23219

[2]Department of Physiology and Biophysics, Virginia Commonwealth University School of Medicine, 1101 East Marshall St, Richmond, Virginia 23298

Abstract

Bioreactors for the reseeding of decellularized lung scaffolds have evolved with various advancements, including biomimetic mechanical stimulation, constant nutrient flow, multi-output monitoring, and large mammal scaling. Although dynamic bioreactors are not new to the field of lung bioengineering, ideal conditions during cell seeding have not been extensively studied or controlled. To address the lack of cell dispersal in traditional seeding methods, we have designed a two-step bioreactor. The first step is a novel system that rotates a seeded lung every 20 minutes at different angles in a sequence designed to anchor 20 percent of cells to a particular location based on the known rate of attachment. The second step involves perfusion-ventilation culture to ensure nutrient dispersion and cellular growth. Compared to statically seeded lungs, rotationally seeded lungs had significantly increased dsDNA content and more uniform cellular distribution after perfusion and ventilation had been administered. The addition of this novel seeding system before traditional culture methods will aid in recellularizing the lung and other geometrically complex organs for tissue engineering.

Keywords

Lung tissue engineering; bioreactor; decellularization; rotation seeding; decellularized scaffold

Introduction

Designing culture methods for 3D tissue engineering requires complex strategies to overcome challenges that do not typically apply to 2D culture. At a minimum, the chosen

[*]Corresponding author: Department of Biomedical Engineering, Virginia Commonwealth University, 800 E. Leigh St, Room 1071, Richmond, VA 23219, rlheise@vcu.edu.

Author Contributions

BMY performed experiments, designed the bioreactor, and wrote portions of the paper. LMA analyzed data and wrote portions of the paper. KS performed experiments, analyzed data and edited the paper. RLH performed experimental design, data analysis, and paper writing and editing.

Declarations of interest: none

Statement of Ethics. Studies involving rat lungs were approved by the VCU Institutional Animal Care and Use Committee (IACUC) under protocol number AD10001468.

Conflict of Interest Statement

Dr. Young is currently employed by Tympanogen, though this work was conducted while she was a student at Virginia Commonwealth University. The other authors have no conflicts of interest to declare.

methods must consider approaches that allow for appropriate cell seeding and nutrient delivery throughout intricate and specialized macro- and micro-architecture of complex organs, especially within the lungs. Fortunately, decellularized lungs come equipped with an ideal route for dispersal through the vast network of airways and vasculature. Still, regenerated lung tissues are far from functioning, and several significant challenges exist, including incomplete cell seeding of the entire scaffold, partial cell differentiation, and lack of uniform organ function. These obstacles hinder lung bioengineering from creating viable transplant alternatives. Improving bioreactor designs and seeding techniques by adding cell-specific dynamic seeding protocols to current methods may help overcome these challenges.

Automated bioreactors are essential for the culture of tissue-engineered constructs to improve several phases of regeneration: 1) cell seeding and dispersal, 2) continuous delivery of fresh nutrients to enhance cell viability, 3) maintenance of a sterile environment with a closed system, and 4) proper timing of biomimetic mechanical stimulus to guide differentiation (Bonvillain et al., 2013; Ott et al., 2010; Raredon et al., 2016). Recent commercially available and custom lung bioreactor systems have advanced further by including artificial pleural membranes, gas exchange units, waste removal, real-time monitoring of oxygen and lung mechanics, and high-throughput automation (Charest et al., 2015; Gilpin et al., 2017; Le et al., 2017; Raredon et al., 2016; Ren et al., 2015). While lung bioreactor development has progressed substantially, our research suggests that fundamental aspects of cell attachment during regeneration have been overlooked in these intricate bioreactor designs.

Two main bioreactor designs for recellularization of acellular lung scaffolds are the perfusion-ventilation bioreactor system and rotating wall vessel (RWV) (Crabbé et al., 2015; Petersen et al., 2010). A perfusion-ventilation bioreactor system provides mechanical ventilation via negative pressure and pulsatile flow of media through the vasculature. Reseeding in this system is typically done either at rest during cell attachment or by constant perfusion of cells into the lung. Alternatively, the RWV bioreactor system applies rotation during culture to increase nutrient dispersal and promote differentiation (Crabbé et al., 2015) without dynamic culture during reseeding. Typically, scaffolds are perfused with cells, sometimes centrifuged, and given time for cells to attach before utilizing the RWV bioreactors. Both of these designs have their limitations due to either cell settling during prolonged static cell attachment periods or cause cell adhesion inhibition because of constant flow. While both systems have made tremendous strides towards developing functional lungs, failure upon transplant and incomplete seeding within histological sections (Gilpin et al., 2014a; Santis et al., 2018) highlight possible insufficient cell dispersal in the first few hours of culture.

Within all bioreactor designs, the appropriate culture parameters can vary drastically depending on the lung regeneration application and donor tissue size. For example, the maximum arterial flow rate for rats is 10-20 mL/min, with a total lung capacity of 10-15 mL (Gilpin et al., 2016a). For larger mammal species such as humans and pigs, arterial flow rates can be 1000 times faster and 700 times larger lung capacity (Protti et al., 2015). Anatomical geometry and intended physiology also must be incorporated. Alveolar recellularization is the main focus of this research as it is the main functional structure of the

lung and the most challenging as the most distal part of the airways. The 200 μm spherical structures require attachment or migration of approximately ten, 20 μm type 1 epithelial cells around the entirety of the sphere (Wikswo et al., 2013). This recellularization approach focuses on guiding attachment throughout all dimensions of all alveolar structures before providing a species-specific flow rate is necessary during cellular differentiation.

The latest advances in both commercially available and custom lung bioreactor systems have extended the length of culture and reproducibility; however, they result in dysfunctional lungs with insufficient cell coverage even after one month of culture (Charest et al., 2015; Nichols et al., 2018). Due to the complex 3D structure, the distribution of the cells within the alveoli and throughout all alveoli may require dynamic seeding regimens at a cell-specific rate (Crabbé et al., 2015). This research proposes a combination of intermittent rotation during cell seeding and perfusion culture to achieve sustained bioengineered lung function and advance tissue engineering methods. After rotation, intermittent resting intervals at systematic angles then allow for cell adhesion complex formation and maturation. Each time rotation is resumed during the initial seeding period, unattached cells are moved to a new region for adherence. Given the importance of maximum attachment of delivered cells throughout recellularized lungs, this study aims to increase cell dispersal using a rotational seeding method for *ex vivo* culture of decellularized lungs. We hypothesize that a 3-hour rotational seeding regimen, followed by overnight static culture, and finally perfusion-ventilation culture on the second day provides the necessary nutrient flow and mechanical stimulation with previously unachieved cell dispersal. Figure 1 gives an overview of the process.

Materials and Methods

Two-Step Bioreactor Design and Preparation

Before recellularization, the lung was rinsed 3 times with PBS with 5% Antibiotic/Antimycotic. All bioreactor components were autoclaved, rinsed with PBS with 5% Antibiotic/Antimycotic for 1 day, and handled within a sterile hood before use. Each lung was perfused intratracheally with 50 x 10^6 MLE12s in 12 mL of media using a hand-driven syringe. Inoculated lungs were either put through both components of the two-step bioreactor to include rotational culture for 3 hours in a 50 ml tube or placed directly into the second component of the two-step bioreactor, the perfusion-ventilation bioreactor chamber, for only static culture overnight. The first component of the rotational seeding system was designed for improved attachment and dispersal of cells within decellularized lung scaffolds. The rotational system supports the 50 mL conical tube containing the lung on two long cylinders (Figure 1). One cylinder was attached to a stepper motor programmed using an Arduino Mega 2560 microcontroller (ATmega2560) to rotate the tissue every 20 minutes for 3 hours. This rotation rate ensures uniform coverage of the airways over 3 hours using the cell coating routine illustrated in Figure 2. This rotation procedure allows attachment at every 45° angle of the lung throughout the entire culture. The degree of rotation between resting positions is large to allow for optimal cell movement throughout the tissue. After 3 hours, the rotationally seeded lungs are transferred to the second component of the two-step bioreactor system, a perfusion-ventilation bioreactor system (Figure 1) for static overnight

culture without vascular or airway media flow. Pulsatile vascular perfusion (CellMax) of media through the pulmonary artery at 2 mL/minute and airway media ventilation at 1 breath/minute with negative pressure created by a syringe pump were initiated for all lungs 24 hours after initial seeding for 24 hours. One-way valves were placed into the breathing loop to allow new media exchange during ventilation.

Decellularization

Male and female Sprague Dawley rat lungs were decellularized by published methods (Pouliot et al., 2016). The trachea and pulmonary artery were cannulated to administer rinses and decellularization reagents. Each day over three days, the lung was perfused a minimum of three times with either 0.1% Triton X-100 (Fisher Scientific), 2% sodium deoxycholate (Sigma), and sodium chloride (Fisher Scientific), or a DNase solution and submerged overnight. The lung was rinsed a minimum of three times with a PBS and penicillin/streptomycin solution after each overnight incubation and before perfusion of the next reagent.

Cell Culture

According to the manufacturer's protocols, mouse alveolar epithelial cells (MLE12, ATCC) were cultured with HITES medium containing 2% fetal bovine serum at 37 °C with 5% CO2.

MLE12 cell attachment rate assay

250,000 cells/cm^2 were seeded onto TCP coated with 0.1 mg/mL porcine lung dECM prepared by protocols previously published by our laboratory (Link et al., 2017; Pouliot et al., 2016; Young et al., 2019, 2020). Every 20 minutes for 4 hours, unadhered cells and media were aspirated from a well and rinsed gently before fixation with 4 % PFA. Cell nuclei were stained using DAPI Prolong Gold Antifade Mounting agent. The number of nuclei was counted within 3 pre-determined regions of each well using a Zeiss AxioObserver Z1 fluorescence microscope. The percent of cell attachment was calculated by dividing the number of cells attached by the number of cells seeded.

Resazurin Reduction Assay

Each lung was perfused for 4 hours with 50 μM resazurin media solution 24 hours after seeding. To reduce contamination early in the culture, a picture of the resazurin color changed was briefly taken with the lung placed on a sterile surface without disconnection from the bioreactor tubing. The lung was perfused again 48 hours later on day 3 by removing all media from the main chamber and again perfusing the lung with 50 μM resazurin media solution. This solution remained within the lung for 4 hours until absorbance (544 nm (ex)/590 nm (em)) levels of the resazurin solution and images were taken to evaluate the metabolic activity of the cells. Absorbance values were subtracted from the non-metabolized stock concentration of the 50 μM resazurin solution.

Histology Imaging and Quantification

Each lung (right or left) was divided transversely into superior and inferior regions, then further divided into anterior or posterior halves. Dissected tissue for histology and other assays were chosen based on resazurin cell viability throughout the lung to isolate regions with similar cell viability for histology and Picogreen. An entire anterior or posterior half of each lung was fixed by submerging the tissue in 4% paraformaldehyde for a minimum of 24 hours. The fixed tissue was then embedded and sectioned through the frontal plane to see the distribution of cells throughout the entirety of the lung, as depicted in Figure 4. Two histological sections, several millimeters apart, were taken from each tissue region for staining with hematoxylin and eosin (H & E) and imaged using a Vectra Polaris Automated Quantitative Pathology Imaging System.

Randomly selected 20x images from five pre-determined regions (top, bottom, right, left, and center) of one histological section were analyzed using Image J. A mask of each image was created with a set threshold range from 50 to 150. This created a binary image containing only the cell nuclei, which was verified by hand counting. After separating touching nuclei and removing any background signal smaller than 15 pixels, the analyzed particles function was used to count the cell number and reported as an average fold change compared to statically seeded lungs.

dsDNA quantification

A Picogreen dsDNA quantification assay (ThermoFisher) was performed according to the manufacturer's protocols on the lungs' remaining portions not used for histological sectioning. Each sample was normalized to its wet weight and graphed as total dsDNA throughout the tissue.

Statistical Analysis

All data are presented as mean +/− standard deviation with an $N \geq 3$ unless otherwise stated. T-tests determined statistical significance between static and rotationally seeded lungs using GraphPad Prism.

Results

Bioreactor design

We have added a novel preliminary bioreactor designed to an existing bioreactor system to enhance cell dispersal and mimic the mechanics within the lungs. The first portion of the bioreactor system is a rotational seeding unit (Figure 1) that turns the lung every 20 minutes in a pattern illustrated in Figure 2 for 3 hours during the initial cell attachment period. Large degrees of rotation were used between resting periods to tumble the cells through multiple regions of the lungs before settling at the desired location. The duration of the resting periods was determined by the rate of MLE12 attachment (Figure 2) to allow 10 percent of cells to attach at each position. This aided in the attachment of cells more evenly throughout the lung. Seeding efficiency was characterized by H & E staining and Picogreen dsDNA quantification. After 3 hours of cell attachment, the lung was moved to the perfusion-ventilation bioreactor (Figure 1) for mechanical conditioning and media

recycling with vascular and airway perfusion. The perfusion-ventilator bioreactor design was adapted from a previously published design (Bonvillain et al., 2013; Calle et al., 2011) without the endothelial seeding chamber.

Resazurin and Picogreen assessment of cell distribution within cultured lungs

50 million MLE12 cells were cultured into decellularized rat lungs with rotational or static seeding conditions to determine if periods of dynamic culture can increase cell dispersal and improve cell retention throughout the lung. Resazurin was perfused through the airways and cultured for 4 hours to allow for metabolites to gradually change the color of the resazurin solution from a dark blue to pink for whole-lung cell viability assessments. After 24 and 72 hours of culture, rotationally seeded lungs exhibited a more uniform pink or light purple color distribution, correlating to viable cells throughout, while static seeding causes several distinct regions with either viable cells (pink) or dark purple to blue (less cellular metabolism, Figure 3). Resazurin absorbance of the lung perfusate (Figure 3) was collected from the tracheal cannula and showed increased cell viability with rotational seeding.

The dsDNA content increased for rotationally seeded lungs compared to statically seeded lungs after 72 hours. Combining the dsDNA concentrations within all areas of each lung showed total dsDNA concentrations (Figure 3) that resembled the results seen by resazurin absorbance, as expected. To better understand where cells are attached with both seeding methods, the distribution of the data points representing the different regions shows large variability. Still, many areas within the static group have a very low concentration.

Cell dispersal within dynamically culture lungs

Histology was also done to verify the findings from resazurin and Picogreen cell distribution studies. After 72 hours of culture (Figure 4), there were distinct cell attachment and distribution differences. Rotational seeding resulted in cells deposited in most regions of the posterior and anterior lungs. In contrast, static seeding caused only a few cells to attach throughout the whole lung and only within a small area. All static lungs had either the anterior or posterior region with much fewer cells suggesting settling according to the force of gravity.

The histological sections' quantification of cell attachment confirms that more cells were deposited across lung regions (Figure 5A) and overall (Figure 5B).

Discussion

Several other researchers have attempted to improv cell seeding methods into biomaterials to enhance whole lung bioengineering. Still, the implementation of these methods has faced unanswered challenges. Typical lung cultures within perfusion -ventilator bioreactor systems start without fluid or air flow for the first 12 hours to 2 days to allow for cell attachment. With this method, gravity and cell settling can drastically affect cell dispersal. Within the same system, cellular seeding has also been done with either vascular or airway media flow, continuously moving cells and media. This method can increase cells' dispersal; however, suspension cultures can disrupt cell attachment rates (Karuri et al., 2004; Nichols et al., 2017). Alternatively, with RWV systems, cells are first perfused throughout the lung, and

then the seeded tissue is statically cultured for 1 to 4 days before initiating rotational culture (Cortiella et al., 2010; Crabbé et al., 2015; Radtke and Herbst-Kralovetz, 2012). This system mainly increases nutrient flow and creates microgravity throughout the culture; however, static seeding causes cell sedimentation and limits cells from spreading from the start. When the RWV system has been used for rotational seeding, the lung itself does not rotate to move cells throughout the airways, and constant rotation at 20 RPM would not give cells time to adhere to the matrix.

In vivo, migratory cells such as immune or metastatic cells require flow to initiate cell adhesion. Laminar flow during epithelial cell seeding can decrease the rate of attachment (Karuri et al., 2004) and even increase metastatic potential (Rizvi et al., 2013). Alternatively, to ensure sufficient epithelial attachment, periods of static culture are required to allow for cell adhesion complexes to be formed. Cells first make attachments to their ECM substrates through integrin-based focal adhesions. Epithelial cells then spread, reorganize their cytoskeleton, and initiate more integrin interactions with the ECM to strengthen adhesion over time. Adhesion complexes begin cooperatively binding after just one minute, but it takes up to 10 to 20 minutes for the cell adhesion structures to withstand substantial shear forces (Taubenberger et al., 2007). Once epithelial attachments have matured, fluid flow and shear stresses become an essential driver of cell differentiation. After attachment, a long-term culture within a perfusion-ventilator bioreactor system is used to distribute nutrients and apply biophysical stimuli. While perfusion-ventilator and RWV systems provide beneficial advanced media dispersal and mechanical cues that aid in tissue maturation, they require refining concerning seeding procedures. The bioreactor design described in this study consolidates these traditional systems' innovative properties while overcoming their limitations in cell dispersal and attachment.

In this study, we have developed a cell seeding protocol to be used in tandem with other long-term culture techniques that increases cell dispersal and overcome the limitations of traditional bioreactor methods. This two-phase culture system includes a rotational cell attachment step to increase cell distribution throughout the lung. This research has focused on alveolar epithelial attachment first to ensure cell distribution can be improved to the vital and most distal regions of the gas-exchange barrier. Over 60 different cell types can be found in the lung with varying attachment and migration characteristics (Price et al., 2010). One group has recognized the importance of attachment rate and harnessing the force of gravity with tissue positioning in improving re-endothelialization of decellularized lungs by placing the lung in a supine position without flow for one hour. However, increased cellular distribution only benefited the posterior half of the larger vessels since the lung was not repositioned, and flow was added after one hour (Stabler et al., 2016). Establishing the attachment rate of MLE12's to decellularized ECM extracts was used to dictate the timing schedule for 20-minute rests before rotation and predict overall cell coverage throughout an alveolar sac over the first phase of culture. A cell- and application-specific attachment assay should be performed to adjust waiting times, speed of the rotation, and resting lung orientation to create custom seeding routines based on the differing cell attachment characteristics. This procedure includes only one application of cells for continuity with other research and to reduce sterility concerns. Division of the cell bolus or multiple applications of the same size may increase the effects of these findings.

Assessing the vitality of graft culture can be difficult without disrupting sterility or progress. Resazurin metabolic assays are an efficient, non-invasive way to evaluate tissue viability during *ex vivo* culture (Gilpin et al., 2016b; Taubenberger et al., 2007; Uzarski et al., 2017). Resazurin reduces to pink-colored resorufin in the presence of cellular metabolites. Pink and purple regions with high cellular viability are easily distinguished from dark blue areas with little cell content. On day 2, after the first cell attachment phase of culture and overnight static culture, it is apparent that statically seeded lungs only had cell viability within a small area of one lung. Rotationally seeded lungs were pink and light purple throughout the regenerating tissue, indicating that more cells survived the culture period and were distributed more evenly throughout all regions of both lungs. After a day of perfusion-ventilator culture, both treatment groups showed a decrease in cell viability, caused by the addition of flow and movement of unattached cells out of the lungs. Yet, lungs seeded with rotation started with more cells attached, resulting in more remaining cells throughout after perfusion-ventilator culture. The trachea is the only location with evidence of cellular activity from external resazurin assessment in statically seeded lungs after 3 days. The perfusate's average resazurin absorbance was also quantified at the end of the culture and showed higher cell viability within rotationally seeded lungs. Picogreen measurements by anatomical region further support that distribution was limited to small regions with static seeding. With these several cell dispersal analyses, we can conclude that alveolar epithelial cells were delivered past larger airways and distributed better with dynamic seeding. This exemplifies why initial cell placement can dictate the overall success regardless of the long-term culture methods to follow.

To confirm these findings, sectioning through the frontal plane with H&E staining of the cultured lung shows a broader distribution of cells throughout dynamically seeded lungs. Alternatively, lungs without rotational seeding have few cells throughout and exhibit sedimentation where they are seen. With all of the cells in a small area of the lung without movement, there is a small surface area of ECM for the large number of cells to attach, leaving many cells to remain in suspension within the airways. Once the fluid flow is introduced in phase two, many more cells have not been allowed to attach in statically seeded lungs and are removed. Even in rotationally seeded lungs with the best cell distribution, it is worth noting that cell clumping and rounded cell morphologies are seen within alveolar and airway spaces. These rounded cells appear to be cells that have not yet attached to the matrix,indicating that longer culture times are needed in the second phase of culture. We observed fewer rounded unattached cells in the rotational seeding; however, this was difficult to quantify given the sparse amount of cells in the statically seeded lungs.

This research aims to develop a bioreactor system that can be used with all future tissue engineering advancements and propel future technologies by starting with an efficient seeding mechanism. Since cellular distribution and attachment were the primary goals of these studies, there are some limitations to the study. The nature of a two-step bioreactor causes challenges regarding sterility. The tissue must be transferred from the rotational seeding container to the conventional bioreactor chamber with this bioreactor design after the seeding period is complete. For that reason, two rotationally seeded lungs experienced contaminations. Future studies should incorporate a design modification to create a fully closed system for the rotational seeding portion and the transfer to the conventional

bioreactor. This study also shows short term cell distribution over 3 days and, therefore, does not provide context for cell migration, proliferation, or differentiation. Extending the culture duration with the addition of recent bioreactor upgrades (Gilpin et al., 2014a), (Nichols et al., 2014), scaffold pre-conditioning (Gilpin et al., 2017; Nichols et al., 2018; Young et al., 2019), multiple cell lineages and differentiation techniques (Ghaedi et al., 2014; Gilpin et al., 2014b; Stabler et al., 2016), and other practices for long-term tissue culture, this system can propel the study of more complex tissue transplantation challenges such as cellular differentiation, barrier integrity, longer-term function.

Conclusions

Careful consideration of epithelial attachment in vitro was used to determine the ideal attachment rate within a whole lung scaffold and improved cell coverage. These studies help inform all types of 3D culture methods and emphasize the need for intermittent motion in cellular seeding. The development of a portable rotation system that is not in direct contact with the lung or media allows for reduced contamination and adaptation of these methods to biomaterial applications. Overall, these are promising results highlighting the importance of dynamic culture in ex vivo cell culture to increase recellularization efficiency.

Funding Sources

This work was funded by NSF CMMI-135162 and NIH R21HL146250. Histological sectioning was performed at the VCU pathology core laboratory, which is supported, in part, by funding from the NIH-NCI Cancer Center Support Grant (P30 CA016059).

Data Availability Statement

All data generated during this study are included in this article or are available upon request by contacting the corresponding author.

References

Bonvillain RW, Scarritt ME, Pashos NC, Mayeux JP, Meshberger CL, Betancourt AM, Sullivan DE, and Bunnell BA (2013). Nonhuman Primate Lung Decellularization and Recellularization Using a Specialized Large-organ Bioreactor. JoVE J. Vis. Exp e50825–e50825. [PubMed: 24378384]

Calle EA, Petersen TH, and Niklason LE (2011). Procedure for Lung Engineering. J. Vis. Exp. JoVE

Charest JM, Okamoto T, Kitano K, Yasuda A, Gilpin SE, Mathisen DJ, and Ott HC (2015). Design and validation of a clinical-scale bioreactor for long-term isolated lung culture. Biomaterials 52, 79–87. [PubMed: 25818415]

Cortiella J, Niles J, Cantu A, Brettler A, Pham A, Vargas G, Winston S, Wang J, Walls S, and Nichols JE (2010). Influence of Acellular Natural Lung Matrix on Murine Embryonic Stem Cell Differentiation and Tissue Formation. Tissue Eng. Part A 16, 2565–2580. [PubMed: 20408765]

Crabbé A, Liu Y, Sarker SF, Bonenfant NR, Barrila J, Borg ZD, Lee JJ, Weiss DJ, and Nickerson CA (2015). Recellularization of Decellularized Lung Scaffolds Is Enhanced by Dynamic Suspension Culture. PLOS ONE 10, e0126846. [PubMed: 25962111]

Ghaedi M, Mendez JJ, Bove PF, Sivarapatna A, Raredon MSB, and Niklason LE (2014). Alveolar epithelial differentiation of human induced pluripotent stem cells in a rotating bioreactor. Biomaterials 35, 699–710. [PubMed: 24144903]

Gilpin SE, Guyette JP, Gonzalez G, Ren X, Asara JM, Mathisen DJ, Vacanti JP, and Ott HC (2014a). Perfusion decellularization of human and porcine lungs: Bringing the matrix to clinical scale. J. Heart Lung Transplant 33, 298–308. [PubMed: 24365767]

Gilpin SE, Ren X, Okamoto T, Guyette JP, Mou H, Rajagopal J, Mathisen DJ, Vacanti JP, and Ott HC (2014b). Enhanced Lung Epithelial Specification of Human Induced Pluripotent Stem Cells on Decellularized Lung Matrix. Ann. Thorac. Surg 98, 1721–1729. [PubMed: 25149047]

Gilpin SE, Charest JM, Ren X, and Ott HC (2016a). Bioengineering Lungs for Transplantation. Thorac. Surg. Clin 26, 163–171. [PubMed: 27112255]

Gilpin SE, Charest JM, Ren X, Tapias LF, Wu T, Evangelista-Leite D, Mathisen DJ, and Ott HC (2016b). Regenerative potential of human airway stem cells in lung epithelial engineering. Biomaterials 108, 111–119. [PubMed: 27622532]

Gilpin SE, Li Q, Evangelista-Leite D, Ren X, Reinhardt DP, Frey BL, and Ott HC (2017). Fibrillin-2 and Tenascin-C bridge the age gap in lung epithelial regeneration. Biomaterials 140, 212–219. [PubMed: 28662401]

Karuri NW, Liliensiek S, Teixeira AI, Abrams G, Campbell S, Nealey PF, and Murphy CJ (2004). Biological length scale topography enhances cell-substratum adhesion of human corneal epithelial cells. J. Cell Sci 117, 3153–3164. [PubMed: 15226393]

Le AV, Hatachi G, Beloiartsev A, Ghaedi M, Engler AJ, Baevova P, Niklason LE, and Calle EA (2017). Efficient and Functional Endothelial Repopulation of Whole Lung Organ Scaffolds. ACS Biomater. Sci. Eng 3, 2000–2010. [PubMed: 33440555]

Link PA, Pouliot RA, Mikhaiel NS, Young BM, and Heise RL (2017). Tunable Hydrogels from Pulmonary Extracellular Matrix for 3D Cell Culture. JoVE J. Vis. Exp e55094–e55094.

Nichols JE, Niles JA, Vega SP, Argueta LB, Eastaway A, and Cortiella J (2014). Modeling the lung: Design and development of tissue engineered macro- and micro-physiologic lung models for research use. Exp. Biol. Med. Maywood NJ 239, 1135–1169.

Nichols JE, La Francesca S, Vega SP, Niles JA, Argueta LB, Riddle M, Sakamoto J, Vargas G, Pal R, Woodson L, et al. (2017). Giving new life to old lungs: methods to produce and assess whole human paediatric bioengineered lungs. J. Tissue Eng. Regen. Med 11, 2136–2152. [PubMed: 26756722]

Nichols JE, Francesca SL, Niles JA, Vega SP, Argueta LB, Frank L, Christiani DC, Pyles RB, Himes BE, Zhang R, et al. (2018). Production and transplantation of bioengineered lung into a large-animal model. Sci. Transl. Med 10, eaao3926. [PubMed: 30068570]

Ott HC, Clippinger B, Conrad C, Schuetz C, Pomerantseva I, Ikonomou L, Kotton D, and Vacanti JP (2010). Regeneration and orthotopic transplantation of a bioartificial lung. Nat. Med 16, 927. [PubMed: 20628374]

Petersen TH, Calle EA, Zhao L, Lee EJ, Gui L, Raredon MB, Gavrilov K, Yi T, Zhuang ZW, Breuer C, et al. (2010). Tissue-Engineered Lungs for in Vivo Implantation. Science 329, 538–541. [PubMed: 20576850]

Pouliot RA, Link PA, Mikhaiel NS, Schneck MB, Valentine MS, Kamga Gninzeko FJ, Herbert JA, Sakagami M, and Heise RL (2016). Development and characterization of a naturally derived lung extracellular matrix hydrogel. J. Biomed. Mater. Res. A n/a-n/a.

Price AP, England KA, Matson AM, Blazar BR, and Panoskaltsis-Mortari A (2010). Development of a Decellularized Lung Bioreactor System for Bioengineering the Lung: The Matrix Reloaded. Tissue Eng. Part A 16, 2581–2591. [PubMed: 20297903]

Protti A, Andreis DT, Milesi M, lapichino GE, Monti M, Comini B, Pugni P, Melis V, Santini A, Dondossola D, et al. (2015). Lung anatomy, energy load, and ventilator-induced lung injury. Intensive Care Med. Exp 3, 34. [PubMed: 26671060]

Radtke AL, and Herbst-Kralovetz MM (2012). Culturing and applications of rotating wall vessel bioreactor derived 3D epithelial cell models. J. Vis. Exp. JoVE

Raredon MSB, Rocco KA, Gheorghe CP, Sivarapatna A, Ghaedi M, Balestrini JL, Raredon TL, Calle EA, and Niklason LE (2016). Biomimetic Culture Reactor for Whole-Lung Engineering. BioResearch Open Access 5, 72–83. [PubMed: 27088061]

Ren X, Moser PT, Gilpin SE, Okamoto T, Wu T, Tapias LF, Mercier FE, Xiong L, Ghawi R, Scadden DT, et al. (2015). Engineering pulmonary vasculature in decellularized rat and human lungs. Nat. Biotechnol 33, 1097–1102. [PubMed: 26368048]

Rizvi I, Gurkan UA, Tasoglu S, Alagic N, Celli JP, Mensah LB, Mai Z, Demirci U, and Hasan T (2013). Flow induces epithelial-mesenchymal transition, cellular heterogeneity and biomarker

modulation in 3D ovarian cancer nodules. Proc. Natl. Acad. Sci 110, E1974–E1983. [PubMed: 23645635]

Santis MMD, Bölükbas DA, Lindstedt S, and Wagner DE (2018). How to build a lung: latest advances and emerging themes in lung bioengineering. Eur. Respir. J 52, 1601355. [PubMed: 29903859]

Stabler CT, Caires LC, Mondrinos MJ, Marcinkiewicz C, Lazarovici P, Wolfson MR, and Lelkes PI (2016). Enhanced Re-Endothelialization of Decellularized Rat Lungs. Tissue Eng. Part C Methods 22, 439–450. [PubMed: 26935764]

Taubenberger A, Cisneros DA, Friedrichs J, Puech P-H, Muller DJ, and Franz CM (2007). Revealing Early Steps of α2β1 Integrin-mediated Adhesion to Collagen Type I by Using Single-Cell Force Spectroscopy. Mol. Biol. Cell 18, 1634–1644. [PubMed: 17314408]

Uzarski JS, DiVito MD, Wertheim JA, and Miller WM (2017). Essential Design Considerations for the Resazurin Reduction Assay to Noninvasively Quantify Cell Expansion within Perfused Extracellular Matrix Scaffolds. Biomaterials 129, 163–175. [PubMed: 28343003]

Wikswo JP, Curtis EL, Eagleton ZE, Evans BC, Kole A, Hofmeister LH, and Matloff WJ (2013). Scaling and systems biology for integrating multiple organs-on-a-chip. Lab. Chip 13, 3496–3511. [PubMed: 23828456]

Young BM, Shankar K, Tho CK, Pellegrino AR, and Heise RL (2019). Laminin-driven Epac/Rapl regulation of epithelial barriers on decellularized matrix. Acta Biomater. 100, 223–234. [PubMed: 31593773]

Young BM, Pouliot RA, Link PA, Park HE, Kahn AR, Shankar K, Schneck MB, Weiss DJ, and Heise RL (2020). Porcine Lung-Derived Extracellular Matrix Hydrogel Properties Are Dependent on Pepsin Digestion Time. Tissue Eng. Part C Methods 26, 332–346. [PubMed: 32390520]

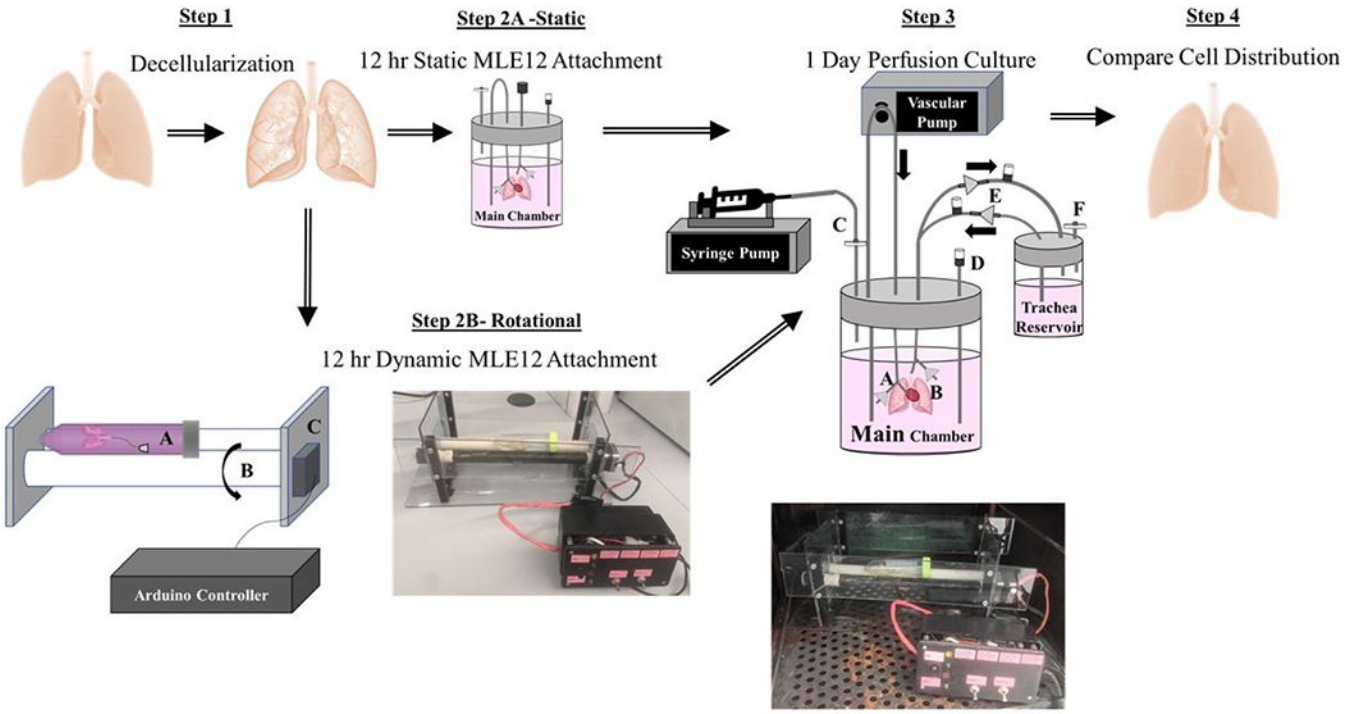

Figure 1. Overview of Cell Seeding and Lung Culture Methods.

Rat lungs were first decellularized over a 3 day period. The resulting scaffolds were either statically or rotationally seeded for 3 hours. Statically-seeded lungs were transferred into the main chamber of the perfusion-ventilation system and left at 37° C overnight. Alternatively, to encourage cell distribution, decellularized lungs were also placed in a 50 mL conical tube (Step 2B, part C) on two cylinders for periodic rotation. A stepper motor (Step 2B, part C) controlled by a programmed Arduino microcontroller rotated one cylinder (Step 2B, part B) and subsequently the lung within the tube systematically every 20 minutes for 3 hours.

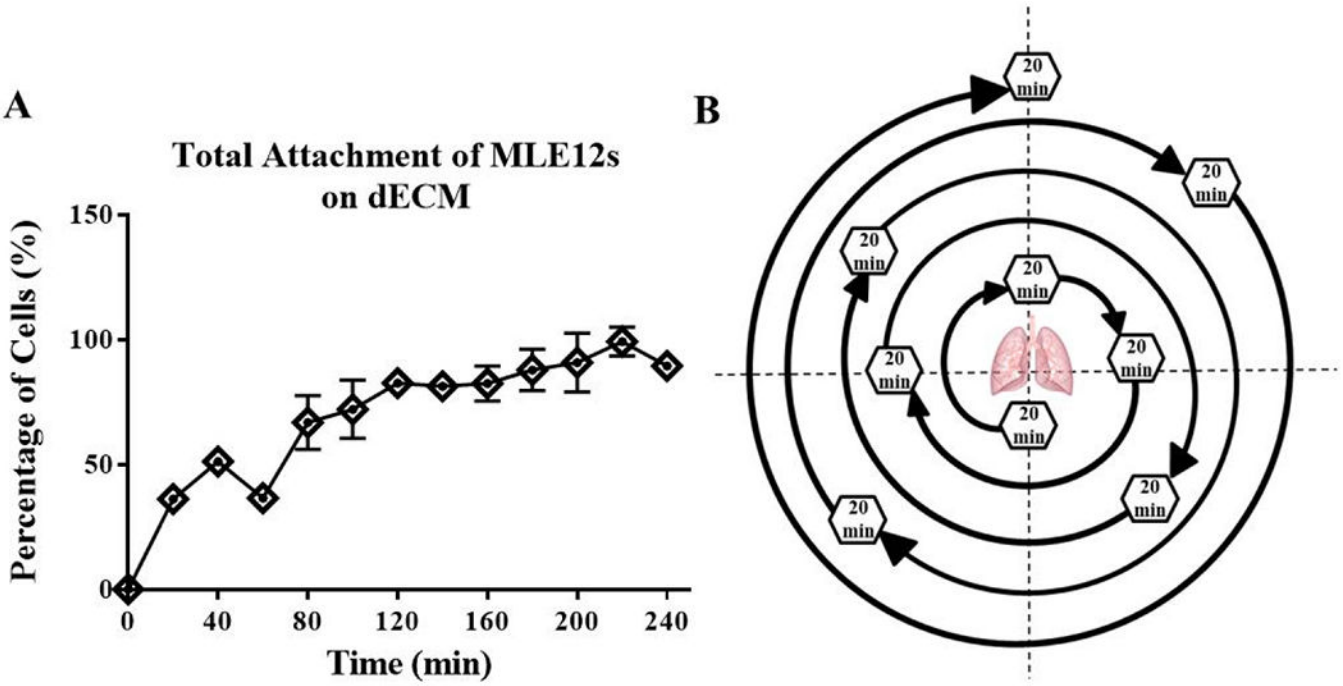

Figure 2. Rotational seeding movement pattern over 3 hours.

The rate of MLE12 cell attachment to TCP coated with lung dECM (A) shows ~15% of cells attach every 20 minutes. The rotation sequence (B) of the cell seeding bioreactor was programmed to ensure every normal plane or 45° angle from the normal plan was rested at over 3 hours by rotating to a new position every 20-minutes. The pattern was chosen systematically with large angles of rotation between each resting position allow for recoating of the cells throughout the lung before reaching its 20 minute resting position. Data are presented as mean from 3 experimental replicates.

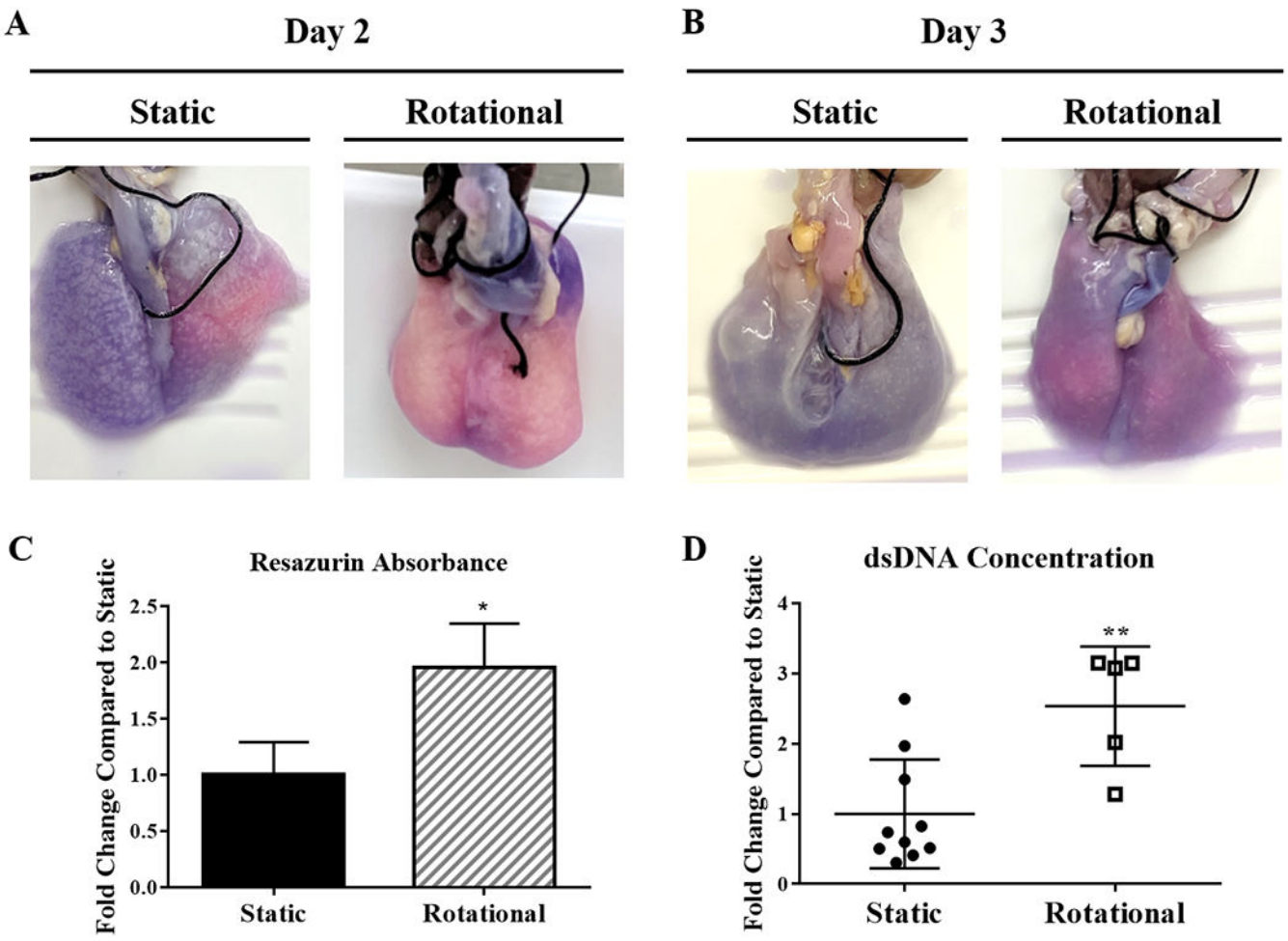

Figure 3. Whole Lung Cellular Distribution.

Images of reseeded lungs after resazurin perfusion at day 2 (A) and day 3 (B). Pink regions show areas with more cellular activity and dark blue/purple areas with fewer cells. Quantification of resazurin absorbance from each set of lungs after 3 days of culture (C). After 3 Days (D), dsDNA quantification compares the concentration distribution between static to rotationally seeded lungs. Each circle or square represents a concentration from either an anterior or posterior portion of each lung. All lungs but one had more than two regions within one lung represented within the data. Data are presented as mean +/− standard deviation from 3 reseeded lungs. *, ** indicates $p < 0.05$, $p < 0.01$ respectively.

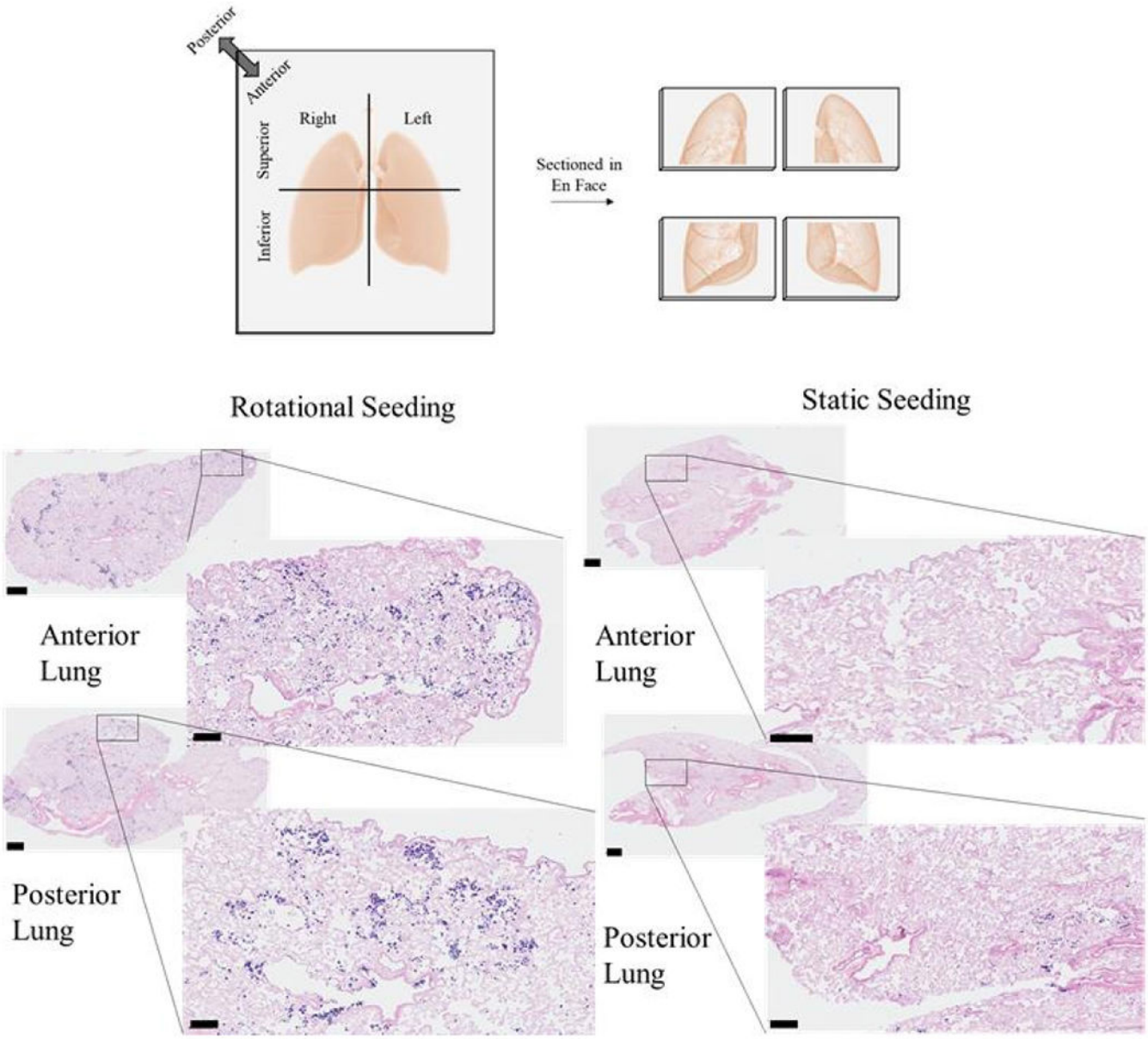

Figure 4. Histological analysis of cell attachment after static or dynamic seeding.

Representative images from the histological sections from either the anterior or posterior regions of the left or right lungs are shown. Scale bars on larger images indicate 100 μm, and scale bars on smaller, magnified images indicate 600 μm.

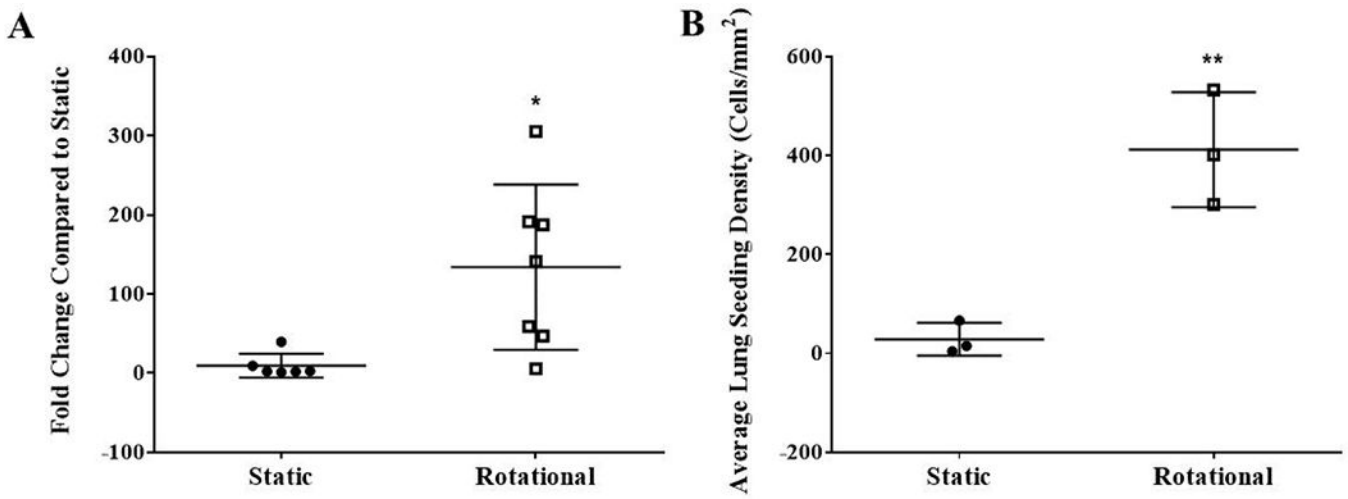

Figure 5. Quantification of cell attachment within histological sections after static or dynamic seeding.

Histological sections within a minimum of 6 different regions (posterior or anterior from the right or left lung) per group of 3 lungs were used to quantify cell attachment. All nuclei within a randomly selected 20x magnification field from 5 different regions of the histological section (top, bottom, left, right, and center) were counted using Image J. The average fold change compared to static was quantified from histological sections of 13 different regions (posterior or anterior from the right or left lung) between 3 lungs per group (A). Each data point represents the average fold change compared to static lungs for each of the 13 lung regions. The average cells/mm^2 within each recellularized lung (B). Data are presented as mean +/− standard deviation. * and ** indicates $p < 0.05$ and $p< 0.01$, respectively.